Thermodynamics of electromechanically coupled mixed ionic-electronic conductors: Deformation potential, Vegard strains, and flexoelectric effect

A. N. Morozovska,[1,*] E. A. Eliseev,[1,2] A. K. Tagantsev,[3] S. L. Bravina,[4] Long-Qing Chen,[5] and S. V. Kalinin[6,†]

[1]*Institute of Semiconductor Physics, National Academy of Science of Ukraine, 41, prospekt Nauki, 03028 Kiev, Ukraine*

[2]*Institute for Problems of Materials Science, National Academy of Science of Ukraine, 3, Krjijanovskogo, 03142 Kiev, Ukraine*

[3]*Ceramics Laboratory, Swiss Federal Institute of Technology (EPFL), CH-1015 Lausanne, Switzerland*

[4]*Institute of Physics, National Academy of Science of Ukraine, 46, prospekt Nauki, 03028 Kiev, Ukraine*

[5]*Department of Materials Science and Engineering, Pennsylvania State University, University Park, Pennsylvania 16802, USA*

[6]*The Center for Nanophase Materials Sciences and Materials Sciences and Technology Division, Oak Ridge National Laboratory, Oak Ridge, Tennessee 37831, USA*

(Received 16 August 2010; revised manuscript received 17 January 2011; published 11 May 2011)

Strong coupling among external voltage, electrochemical potentials, concentrations of electronic and ionic species, and strains is a ubiquitous feature of solid state mixed ionic-electronic conductors (MIECs), the materials of choice in devices ranging from electroresistive and memristive elements to ion batteries and fuel cells. Here, we analyze in detail the electromechanical coupling mechanisms and derive generalized bias-concentration-strain equations for MIECs including contributions of concentration-driven chemical expansion, deformation potential, and flexoelectric effect. This analysis is extended toward the bias-induced strains in the uniform and scanning-probe-microscopy-like geometries. Notably, the contribution of the electron-phonon and flexoelectric coupling to the local surface displacement of the mixed ionic-electronic conductor caused by the electric field scanning probe microscope tip has not been considered previously. The developed thermodynamic approach allows evolving the theoretical description of mechanical phenomena induced by the electric fields (electromechanical response) in solid state ionics toward analytical theory and phase-field modeling of the MIECs in different geometries and under varying electrical, chemical, and mechanical boundary conditions.

DOI: 10.1103/PhysRevB.83.195313 PACS number(s): 72.60.+g, 66.30.Qa

I. INTRODUCTION

Development of strains is a phenomenon ubiquitous in solid-state electrochemical devices including batteries,[1,2] fuel cells[3,4] and electroresistive and memristive electronics. For example, strain is one of the dominant factors contributing to the mechanical instability of solid oxide fuel cells and Li-ion battery anodes such as intraparticle cracking and delamination of electrodes.[5,6] The difference in boundary conditions (clamped or unclamped material) can significantly shift the electrochemical potentials of reacting species and electrons[7] and affect charge-discharge hysteresis and hence efficiency of materials and devices. On the other hand, electrochemically generated strains can be utilized to build electromechanical devices such as artificial muscles[8] and actuators,[9] or diagnostic tools for electrochemical systems at both the macroscopic[10] and nanometer scales.[11] Electrochemical strain microscopy[11,12] uses the periodic nanoscale electrochemical strains generated by a biased scanning probe of microscope to detect Li-ion diffusion in cathode[13] and anode materials[14] at the 10–100 nm scale. Based on the previous imaging and spectroscopy results in ferroelectric materials,[15–17] it is possible to perform electrochemical strain microscopy measurements at the level of several nanometers, opening the pathway for probing structure-electrochemical property relationships at a single structural defect.

A common source for strain in electrochemically active materials is the compositional dependence of lattice parameters, as discussed in detail by Larche and Cahn.[18] This is the case for many ionic and mixed ionic-electronic conductors such as ceria,[19] cobaltites,[20–23] nikelates,[24] and manganites.[25] Similarly, insertion and extraction of Li ions in Li-battery electrodes produce large volume changes.[26,27] Most of the previous theoretical studies of strain effects in diffusional[28,29] and electrochemical systems consider this compositional lattice expansion as the only source of strain. This assumption is reasonable if the electronic conductivity of a material is sufficiently high to avoid significant potential drops (equivalent to the presence of support electrolyte in liquid electrochemistry[30,31]), obviating electromigration transport and providing local electroneutrality.

However, the situation can differ significantly for the case of materials with finite electronic conductivity, in which both concentration fields and electrostatic field are nonuniform within the material. Electrostatic fields in the material give rise to strains due to electrostriction[32–35] and space-charge[36] effects. Second, the changes in the redox state of Jahn-Teller-(JT-)active cations can give rise to additional strain coupling mechanisms through the deformation potential.[37–42] As an example, in perovskites these effects can be understood as a consequence of the changes in favored oxygen octahedral geometry as a function of oxidation state of the central cation. Similarly to the fact that change in the *d*-orbital population changes octahedral shape and gives rise to the JT effect, the strain-deforming octahedron will shift the electrochemical potential of the central atom. These effects will be particularly pronounced on the nanometer scale as relevant to scanning probe microscopy imaging[43] and nanoparticle/nanowire materials, in which the conditions of local electroneutrality are violated on the length scales of corresponding screening lengths and large (compared to macroscopic systems) strains can be supported.

Inhomogeneous electric fields, which are inevitably present in systems with inhomogeneous space charge (e.g., in the vicinity of the tip-surface junction), induce elastic strains linearly proportional to the field gradient due to the flexoelectric coupling; vice versa, inhomogeneous elastic stress causes electric polarization. The existence of such effects was pointed out by Mashkevich and Tolpygo[44] and Kogan.[45] A comprehensive theory of the flexoelectric effect was offered by Tagantsev,[46–48] experimental measurements of flexoelectric tensor components in bulk crystals were carried out for perovskites by Ma and Cross[49–53] and Zubko *et al.*[54] Further theoretical developments of the flexoelectric response of different nanostructures were made by Catalan *et al.*[55,56] Majdoub *et al.*,[57] Kalinin and Meunier,[58] Eliseev *et al.*,[59] and Sharma *et al.*[60,61]

In this paper, we develop the equilibrium strain-concentration-bias equations for electrochemically active materials that account for chemical expansivity, deformation potential, and flexoelectric effects. The relevant comparison here is the Ginzburg-Landau-type theories for ferroelectric materials that are broadly available for ferroelectrics and allow domain structures,[63] domain dynamics,[62] behavior in nonuniform systems (e.g., strained films and multilayers[63]), and the effects of individual and multiple defects to be explored.[64] Once available for electrochemical systems, similar advances based on phase-field-type models could be achieved.[65–68]

II. GENERALIZED CONCENTRATION-STRAIN-BIAS CONSTITUTIVE RELATION

Here, we analyze the coupling between electrochemical potential and strain in mixed ionic-electronic conductors (MIECs). We consider the flexoelectric effect, deformation potential, quasi-Fermi-level shift by electron-phonon coupling, and Vegard expansion of the lattice caused by mobile donors (and/or acceptors) as the primary contributing mechanisms.

A. Flexoelectric effect contribution to electrostatic potential and elastic stress

For centrosymmetric crystals (considered hereinafter) the *direct* flexoelectric effect gives the equation of state for dielectric polarization $P_i(\mathbf{r})$:[46,47]

$$P_i = \gamma_{klij}\frac{\partial u_{kl}}{\partial x_j} + \varepsilon_0\chi_{ij}E_j, \tag{1}$$

which includes the "flexoelectric" polarization $\gamma_{ijkl}\partial u_{jk}/\partial x_l$ induced by the inhomogeneous strain $u_{ij}(\mathbf{r})$ gradient $\partial u_{ij}/\partial x_l$,[47,53,54] and dielectric response $\varepsilon_0(\varepsilon_{ij}-\delta_{ij})E_j$, where ε_0 is the universal vacuum dielectric constant, $\chi_{ij}=(\varepsilon_{ij}-\delta_{ij})$ is the lattice susceptibility tensor, ε_{ij} is the lattice permittivity tensor, and E_i is the electric field. The flexoelectric strain tensor γ_{ijkl} has been measured experimentally for several substances and it was found to vary by several orders of magnitude from 10^{-11} to 10^{-6} C/m.[69] Hereafter we use the Einstein summation convention for all repeating indices.

Direct substitution of the polarization (1) into the Maxwell equation $\mathrm{div}(\mathbf{P}+\varepsilon_0\mathbf{E})=\rho_f$ along with the definition $E_k(\mathbf{r})=-\partial\varphi(\mathbf{r})/\partial x_k$ leads to the Poisson-type equation with a flexoelectric term for the electric potential $\varphi(\mathbf{r})$ of the MIEC:

$$\varepsilon_0\varepsilon_{ij}\frac{\partial^2\phi(\mathbf{r})}{\partial x_i\partial x_j} = -q[p(\mathbf{r})-n_C(\mathbf{r})-N_a^-(\mathbf{r})+N_d^+(\mathbf{r})] + \gamma_{ijkl}\frac{\partial^2 u_{ij}(\mathbf{r})}{\partial x_k\partial x_l}. \tag{2}$$

Here q is the absolute value of the electron charge, $n_C(\mathbf{r})$ is the concentration of electrons in the conduction band, $p(\mathbf{r})$ is the concentration of holes in the valence band, $N_d^+(\mathbf{r})$ is the concentration of mobile ionized donors, and $N_a^-(\mathbf{r})$ is the concentration of mobile ionized acceptors in the MIEC.

The *converse* flexoelectric effect contributes to Hooke's law relating the strain $u_{kl}(\mathbf{r})$ and stress tensor $\sigma_{kl}(\mathbf{r})$:[70]

$$\sigma_{ij}(\mathbf{r}) = c_{ijkl}u_{kl}(\mathbf{r}) + f_{ijkl}\frac{\partial P_k(\mathbf{r})}{\partial x_l}. \tag{3a}$$

Here c_{ijkl} is the tensor of elastic stiffness and the flexoelectric stress tensor $f_{ijkl}=\gamma_{ijmk}\chi_{ml}^{-1}/\varepsilon_0$. Hereafter we neglect the quadratic contribution of the flexoelectric effect and using Eq. (1) rewrite Eq. (3a) as[71]

$$\sigma_{ij}(\mathbf{r}) = c_{ijkl}u_{kl}(\mathbf{r}) + \gamma_{ijmk}\frac{\partial E_k(\mathbf{r})}{\partial x_m}. \tag{3b}$$

The substitution of the polarization from Eq. (1) into Eq. (3b) leads to the relations

$$\sigma_{ij}(\mathbf{r}) = c_{ijkl}u_{kl}(\mathbf{r}) - \gamma_{ijkl}\frac{\partial^2\varphi(\mathbf{r})}{\partial x_k\partial x_l}, \tag{4a}$$

$$u_{ij}(\mathbf{r}) = s_{ijkl}\sigma_{kl}(\mathbf{r}) + s_{ijmn}\gamma_{mnkl}\frac{\partial^2\varphi(\mathbf{r})}{\partial x_k\partial x_l}, \tag{4b}$$

where $\gamma_{ijkl}\partial^2\varphi(\mathbf{r})/\partial x_k\partial x_l$ is the linear contribution of the flexoelectric effect, and s_{ijkl} is the tensor of elastic compliances.

B. Vegard expansion of the lattice caused by mobile donors and acceptors

The effect of the stoichiometry on the local strain is the *linear* dependence of lattice constants on the chemical composition of the solid solution (Vegard law of chemical expansion[18,72]). In accordance with the Vegard law the local stress σ_{ij} and strains u_{ij} produced by the mobile ion (donors or acceptors) migration and diffusion are related as[1,29]

$$\sigma_{ij} = c_{ijkl}u_{kl}(\mathbf{r}) - \beta_{ij}^d[N_d^+(\mathbf{r})-N_{d0}^+] - \beta_{ij}^a[N_a^-(\mathbf{r})-N_{a0}^-], \tag{5a}$$

$$u_{ij} = s_{ijkl}\sigma_{kl}(\mathbf{r}) + \tilde{\beta}_{ij}^d[N_d^+(\mathbf{r})-N_{d0}^+] + \tilde{\beta}_{ij}^a[N_a^-(\mathbf{r})-N_{a0}^-], \tag{5b}$$

where $N_d^+(\mathbf{r})$ is the instant concentration of mobile ionized donors, $N_a^-(\mathbf{r})$ is the instant concentration of mobile ionized acceptors, N_{d0}^+ and N_{a0}^- are their stoichiometric equilibrium concentrations, and $\beta_{ij}^{a,d}$ and $\tilde{\beta}_{ij}^{a,d}=s_{ijkl}\beta_{kl}^{a,d}$ are the *Vegard expansion* tensors for acceptors (donors).

The structure of the Vegard expansion tensor is controlled by the symmetry (crystalline or Curie group symmetry) of the material; for isotropic or cubic media it is diagonal and reduces to a scalar $\beta_{jk}^{a,d}=\beta^{a,d}\delta_{jk}$ (hereafter δ_{jk} is the Kronecker delta

symbol). Experimental methods for β_{ij} determination are relatively well established. For instance, one could either directly study the strain of a given sample with the changes of stoichiometry (see, e.g., Refs. 23–25) or consider the set of several samples with slightly different compositions (solid solution).

Note that the Vegard strain caused by mobile donors and acceptors leads to the shift of their chemical potential levels proportional to the convolution $\beta^a_{jk}u_{jk}(\mathbf{r})$ or $\tilde{\beta}^a_{jk}\sigma_{jk}(\mathbf{r})$ (see, e.g., Ref. 1) and their equilibrium concentrations in the Boltzmann-Planck-Nernst approximation:

$$N_d^+(\mathbf{r}) \approx N_{d0}^+ \exp\left(\frac{\beta^d_{jk}u_{jk}(\mathbf{r}) - q\varphi(\mathbf{r})}{k_BT}\right), \tag{6a}$$

$$N_a^-(\mathbf{r}) \approx N_{a0}^- \exp\left(\frac{\beta^a_{jk}u_{jk}(\mathbf{r}) + q\varphi(\mathbf{r})}{k_BT}\right), \tag{6b}$$

where $k_B = 1.3807 \times 10^{-23}$ J/K and T is the absolute temperature.

Consequently, Eqs. (5) and (6) can be interpreted as the direct and converse Vegard effects: the ion concentration variation induces stress or strain (the *direct Vegard effect*), or the strain or stress produces the concentration changes (the *converse Vegard effect*).

C. Electron-phonon coupling contribution in the elastic subsystem

In deformation potential theory,[37–42] the strain-induced conduction (valence) band edge shift is proportional to the strain in the linear approximation, namely,

$$\begin{aligned} E_C(u_{ij}(\mathbf{r})) &= E_C(0) + \Xi^C_{ij}u_{ij}(\mathbf{r}), \\ E_V(u_{ij}(\mathbf{r})) &= E_V(0) - \Xi^V_{ij}u_{ij}(\mathbf{r}), \end{aligned} \tag{7}$$

where E_C and E_V are the energetic positions of the bottom of the conduction band and the top of the valence band, respectively,[73] and $\Xi^{C,V}_{ij}$ is the tensor deformation potential of electrons in the conduction (C) and valence bands (V).[40] The properties of the deformation potential tensor $\Xi^{C,V}_{ij}$ are determined by the crystalline symmetry of the material and the positions of the bottom of the conduction band and the top of the valence band in the Brillouin zone.[37–42]

Neglecting the strain-induced changes in the density of states (DOS) in the energy bands, one can express the impact on the strain of the equilibrium concentration of the electrons in the conduction and holes in the valence bands in terms of the introduced deformation potential:[74,75]

$$n_C(\mathbf{r}) = \int_{-\infty}^{\infty}\left[1 + \exp\left(\frac{\varepsilon + E_C + \Xi^C_{ij}u_{ij}(\mathbf{r}) - E_F - q\varphi(\mathbf{r})}{k_BT}\right)\right]^{-1} g_C(\varepsilon)\,d\varepsilon \approx n_{C0}\exp\left(\frac{-\Xi^C_{ij}u_{ij}(\mathbf{r}) + q\varphi(\mathbf{r})}{k_BT}\right), \tag{8a}$$

$$p(\mathbf{r}) = \int_{-\infty}^{\infty}\left[1 + \exp\left(-\frac{\varepsilon + E_V - \Xi^V_{ij}u_{ij}(\mathbf{r}) - E_F - q\varphi(\mathbf{r})}{k_BT}\right)\right]^{-1} g_V(\varepsilon)\,d\varepsilon \approx p_0\exp\left(\frac{-\Xi^V_{ij}u_{ij}(\mathbf{r}) - q\varphi(\mathbf{r})}{k_BT}\right), \tag{8b}$$

where $k_B = 1.3807 \times 10^{-23}$ J/K, T is the absolute temperature, E_F is the Fermi level, and q is the absolute value of the electron charge. The functions $g_m(x)$ with the subscript $m = C, V$ are the densities of states.[76]

Approximate equalities in Eq. (8) correspond to the Boltzmann-Planck-Nernst approximation that is widely used for MIECs (see, e.g., Riess *et al.*[77–79]). In this approximation, in the absence of external potential and strains the equilibrium concentrations of the electrons in the conduction band and holes in the valence band, n_{C0} and p_0, read

$$n_{C0} = \int_{-\infty}^{\infty} d\varepsilon g_C(\varepsilon)\exp\left(\frac{-E_C + E_F - \varepsilon}{k_BT}\right)$$

and

$$p_0 = \int_{-\infty}^{\infty} d\varepsilon g_V(\varepsilon)\exp\left(\frac{E_V - E_F + \varepsilon}{k_BT}\right),$$

respectively.

One readily shows that a converse effect to that discussed above (i.e., the stress or strain produced by the carrier redistribution), conditioned by the deformation potential, should exist, namely,

$$\sigma_{ij}(\mathbf{r}) = c_{ijkl}u_{kl}(\mathbf{r}) + \Xi^C_{ij}[n_C(\mathbf{r}) - n_{C0}] + \Xi^V_{ij}[p(\mathbf{r}) - p_0], \tag{9a}$$

$$u_{ij}(\mathbf{r}) = s_{ijkl}\sigma_{kl}(\mathbf{r}) - \tilde{\Xi}^C_{ij}[n_C(\mathbf{r}) - n_{C0}] - \tilde{\Xi}^V_{ij}[p(\mathbf{r}) - p_0], \tag{9b}$$

The deformation potential tensors in Eqs. (9a) and (9b) are related as $\tilde{\Xi}^{C,V}_{ij} = s_{ijkl}\Xi^{C,V}_{kl}$.

Let us demonstrate the validity of Eq. (9a) for the electrons in the conduction band, obeying the classical statistics. We start from the expression for the free energy density of electrons in the conduction band:[74]

$$\frac{F}{V} = \frac{1}{V}\sum_{\alpha}\{f_\alpha[E_C(u_{ij}) + \varepsilon_\alpha] + k_BT(f_\alpha \ln f_\alpha - f_\alpha)\}. \tag{10a}$$

The summation In Eq. (10a) is performed over the many states in the conduction band denoted by the summation index α. Here

$$f_\alpha = \exp\left(-\frac{E_C(u_{ij}) + \varepsilon_\alpha - E_F - q\varphi}{k_BT}\right) \tag{10b}$$

is the probability of the occupation of the αth state in the band by an electron, the summation is performed over the conduction band, and V is the system volume. Alternatively, $\sum_\alpha f_\alpha$ can be expressed in terms of the density of the electrons,

n_C, and the density of states N_C in the conduction band:

$$n_C = \frac{1}{V}\sum_\alpha f_\alpha \equiv N_C \exp\left(-\frac{E_C - E_F - q\varphi}{k_B T}\right), \quad (10c)$$

Comparing (10b) and (10c) one immediately sees that

$$f_\alpha = \frac{n_C}{N_C}\exp\left(-\frac{\varepsilon_\alpha}{k_B T}\right). \quad (10d)$$

Using (10d) and (10c), the free energy density (10a) can be expressed in terms of its independent variables u_{ij},n_C, and T:

$$\frac{F}{V} = n_C\left\{E_C + k_B T\left[\ln\left(\frac{n_C}{N_C}\right) - 1\right]\right\}. \quad (10e)$$

By definition

$$\sigma_{ij} = \frac{\partial}{\partial u_{ij}}\left(\frac{F}{V}\right)\Big|_{T,n_C} = n_C\left(\frac{\partial}{\partial u_{ij}}E_C(u_{ij}) - \frac{k_B T}{N_C}\frac{\partial N_C}{\partial u_{ij}}\right)$$
$$= n_C \Xi^C_{ij} - n_C\frac{k_B T}{N_C}\frac{\partial N_C}{\partial u_{ij}} \approx n_C \Xi^C_{ij}. \quad (11)$$

Thus, neglecting the strain dependence of the density of states N_C in Eq. (11), and keeping in mind that we are interested in the strain difference between the initial state of the system and that with a changed electron density, we arrive at the second term on the right-hand side of Eq. (9a). The calculations for the stress induced by the variation of the hole density are similar. The impact of the last term, $n_C(k_B T/N_C)(\partial N_C/\partial u_{ij})$, appeared small for semiconductors, since the strain dependence of the effective mass is typically much smaller than the band gap dependence determined by the deformation potential (see, e.g., Ref. 80).

III. ELASTIC FIELDS: FLEXOELECTRIC, VEGARD, AND ELECTRON-PHONON CONTRIBUTIONS

The total stress contains a flexoelectric contribution in accordance with Eq. (4), a Vegard contribution in accordance with Eq. (5), and an electron-phonon contribution in accordance with Eq. (9). Thus, the strain and stress tensors are related as

$$\sigma_{ij}(\mathbf{r}) = c_{ijkl}u_{kl}(\mathbf{r}) + \left\{\Xi^C_{ij}[n_C(\mathbf{r}) - n_{C0}] + \Xi^V_{ij}[p(\mathbf{r}) - p_0] - \beta^a_{ij}[N^-_a(\mathbf{r}) - N^-_{a0}] - \beta^d_{ij}[N^+_d(\mathbf{r}) - N^+_{d0}]\right\} - \gamma_{ijkl}\frac{\partial^2\varphi}{\partial x_k \partial x_l}. \quad (12a)$$

The strain tensor can be expressed via the stress tensor (10) as

$$u_{ij}(\mathbf{r}) = s_{ijkl}\sigma_{kl}(\mathbf{r}) + \left\{\tilde\beta^a_{ij}[N^-_a(\mathbf{r}) - N^-_{a0}] + \tilde\beta^d_{ij}[N^+_d(\mathbf{r}) - N^+_{d0}] - \tilde\Xi^C_{ij}[n_C(\mathbf{r}) - n_{C0}] - \tilde\Xi^V_{ij}[p(\mathbf{r}) - p_0]\right\} + \tilde\gamma_{ijkl}\frac{\partial^2\varphi(\mathbf{r})}{\partial x_k \partial x_l}. \quad (12b)$$

The inverse effect tensors and flexoelectric coefficients in Eq. (11b) are introduced as

$$\tilde\Xi^{C,V}_{ij} = s_{ijkl}\Xi^{C,V}_{kl}, \quad \tilde\beta^{a,d}_{ij} = s_{ijkl}\beta^{a,d}_{kl}, \quad \tilde\gamma_{ijkl} = s_{ijmn}\gamma_{mnkl}. \quad (13a)$$

Note that Eqs. (12) require the reference lattice determination. The reference lattice is regarded as strain-free for the case of zero electric potential, $\varphi = 0$, and therefore

$$n_C(\mathbf{r}) = n_{C0}, \quad p(\mathbf{r}) = p_0, \quad N^-_a(\mathbf{r}) = N^-_{a0}, \quad N^+_d(\mathbf{r}) = N^+_{d0}.$$

Considering the case of isotropic media, for which $\Xi^{C,V}_{ij} = \Xi^{C,V}\delta_{ij}$, $\beta^{a,d}_{ij} = \beta^{a,d}\delta_{ij}$, and $\gamma_{ijkl} = \gamma_D\delta_{ij}\delta_{kl} + \gamma_S(\delta_{ik}\delta_{jl} + \delta_{il}\delta_{jk})$, in Voigt notation Eq. (13a) can be simplified as

$$\tilde\Xi^{C,V}_{ij} = \Xi^{C,V}(s_{11} + 2s_{12})\delta_{ij}, \quad \tilde\beta^{a,d}_{ij} = \beta^{a,d}(s_{11} + 2s_{12})\delta_{ij},$$
$$\tilde\gamma_{33} = \tilde\gamma_{22} = \tilde\gamma_{11} = s_{11}\gamma_{11} + 2s_{12}\gamma_{12}, \quad (13b)$$
$$\tilde\gamma_{12} = \gamma_{11}s_{12} + \gamma_{12}(s_{11} + s_{12}), \quad \tilde\gamma_{44} = \gamma_{44}s_{44}.$$

Note that the group of k at the Γ point in the Brillouin zone is isomorphic to the point group of the lattice so the Γ point has full crystal symmetry. The Γ point symmetry determines the deformation potential tensor.[40] Thus nondiagonal components of the deformation potential tensor as well as of the Vegard strain tensor are possible only for monoclinic and triclinic symmetry materials (since these tensors are symmetric polar ones, their symmetry properties are the same as for, e.g., dielectric susceptibility tensors; see, e.g., Ref. 81).

Estimation of the deformation potential tensor trace performed in the Tomas-Fermi approximation[37] yields the magnitude of $\beta \sim 1$ eV and $\tilde\beta \sim 10^{-30}$ m^3 for Li-containing ionics.[23,25,82] Unfortunately, the Tomas-Fermi approximation can significantly underestimate the deformation tensor value for many materials by up to an order of magnitude.[37,73] Experimental values are not available, albeit they are probably accessible for density-functional-type modeling. In comparison, for Si- or Ge-based semiconductors experimental values are $\tilde\Xi \sim 5{-}10$ eV and $\tilde\Xi \sim (1{-}5)\times 10^{-30}$ m^3.[40,83] Using the values and typical range of concentration variations, namely, (a) 1% deviation from the stoichiometric concentration 10^{28} m^{-3} for ions which gives $[N^-_a(\mathbf{r}) - N^-_{a0}] \sim 10^{26}$ m^{-3}; (b) 10%−100% deviation of electron and hole concentrations in the depletion/accumulation regions which is about $[p_0 - p(\mathbf{r})] \sim 10^{27}$m^{-3}, we estimate that the contributions of the Vegard effect $\tilde\beta^a_{ij}[N^-_a(\mathbf{r}) - N^-_{a0}]$ and deformation potential $\tilde\Xi^V_{ij}[p_0 - p(\mathbf{r})]$ in Eq. (11) are comparable for ionics.

IV. THE STRAIN-VOLTAGE RESPONSE IN THE DECOUPLING APPROXIMATION

Here, we illustrate the contribution of ion and electron migration in the applied electric field to the strain response of the MIEC surface. It is seen from Eqs. (12) that the Vegard expansion, deformation potential, and flexoelectric effect couple the stress field with the carrier distribution, requiring the solution of a fully coupled problem. However, in most cases the changes of the band structure due to the external pressure are rather weak [e.g., for Ge the band gap changes only by about 1% for a rather high strain of about 10^{-3} (Ref. 38)]. Hence, when calculating the space charge distributions the stress contribution can be neglected in the first approximation. Then the ionic and electrostatic field distributions are substituted in Eqs. (12) to yield mechanical responses.

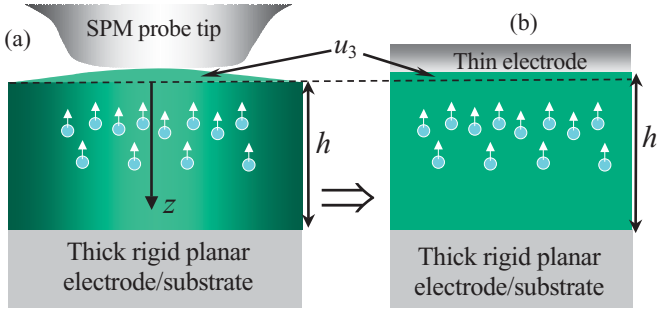

FIG. 1. (Color online) Schematics of ESM measurements with a flattened scanning probe microscope (SPM) tip (a) is approximated by the (b) strain response of the 1D system, where u_3 is the surface displacement for fixed back interface. Voltage V_0 is applied to the top electrode; h is the thickness of MIEC film.

A. Electrochemical strain microscopy of the MIEC

Both ionic and electronic contributions to the local strain can be measured and distinguished by electrochemical strain microscopy (ESM).[11–14,84] For the ionically blocking tip electrode, the electron transfer between the tip and the surface and nonuniform electrostatic field result in the redistribution of mobile ions and electrons within the solid, but no electrochemical process at the interface occurs.[12] The schematic of the system is shown in Fig. 1(a).

A Lamé-type equation for the mechanical displacement u_i can be obtained from the equation of mechanical equilibrium $\partial\sigma_{ij}(\mathbf{r})/\partial x_i = 0$, where the stress tensor $\sigma_{ij}(\mathbf{r})$ is given by Eq. (11a), namely,

$$c_{ijkl}\frac{\partial^2 u_k}{\partial x_j \partial x_l} = -\frac{\partial}{\partial x_j}\left\{ -\beta^a_{ij}[N^-_a(\mathbf{r}) - N^-_{a0}] - \beta^d_{ij}[N^+_d(\mathbf{r}) - N^+_{d0}] - \gamma_{ijkl}\frac{\partial^2\varphi}{\partial x_k \partial x_l} + \Xi^C_{ij}[n_C(\mathbf{r}) - n_{C0}] + \Xi^V_{ij}[p(\mathbf{r}) - p_0]\right\}. \quad (14)$$

Mechanical boundary conditions[85] corresponding to the ESM experiments[11] are defined on the mechanically free interface $z = 0$, where the normal stress σ_{3i} is absent, and on the clamped interface $z = h$, where the displacement u_i is fixed:

$$\sigma_{3i}(x,y,z=0) = 0, \quad u_i(x,y,z=h) = 0. \quad (15)$$

Hereafter we define $x \equiv x_1, y \equiv x_2, z = x_3$ as well as associating the indices $1 \equiv x, 2 \equiv y, 3 = z$ with vector and tensor components.

The tip-bias-induced displacement of the MIEC surface at the point $x_3 = 0$, i.e., surface displacement at the tip-surface junction detected by SPM electronics, for elastically isotropic semispace can be calculated in the decoupling approximation,[12] using the appropriate tensorial Green function for elastic semispace (listed in, e.g., Ref. 86) or thin film (derived in Refs. 87 and 88). The decoupling approximation regards the flexoelectric effect and strain contribution as small enough not to perturb the electrostatic potential and carrier distributions in the first approximation. Thus below we determine the electric potential from Eq. (2) with carrier distributions (6) and (8) without strain terms and then substitute the potential and carrier distribution into Eq. (14).

Note, that the decoupling approximation introduced earlier for the piezoresponse force microscopy (PFM) is sufficiently rigorous for materials with low electromechanical coupling coefficients,[89,90] i.e., for all nonpiezoelectrics considered in the paper. The accuracy of the decoupling approximation is proportional to the square of the electromechanical coupling coefficients, which generally does not exceed 10^{-2} for nonferroelectrics.

B. Strain response of the surface layers

The schematic of the capacitorlike structure that models a disklike SPM tip is illustrated in Fig. 1(b). We consider a MIEC film of thickness h sandwiched between the planar electrodes. For the strain measurements, the top electrode is considered to be mechanically free (e.g., ultrathin, or liquid, or soft polymer), so that its motion does not affect significantly the mechanical displacement of the MIEC film surface. The voltage V_0 is applied to the top electrode; the bottom electrode is earthed:

$$\varphi(z) = V_0 \approx \text{const}, \quad \varphi(h) = 0. \quad (16)$$

The voltage drop between the top and bottom electrodes causes the one-dimensional (1D) redistribution of the carrier concentration in the z direction.

The solution of the system (14)–(15) gives the equilibrium mechanical displacement of the MIEC surface caused by the flexoelectric, electronic and ionic contributions:

$$u_3(z=0) = -\int_0^h dz \left(\left(\tilde{\Xi}^C_{33} - \frac{2s_{12}\tilde{\Xi}^C_{11}}{s_{11}+s_{12}} \right)[n_C(z) - n_{C0}] + \left(\tilde{\Xi}^V_{33} - \frac{2s_{12}\tilde{\Xi}^V_{11}}{s_{11}+s_{12}} \right)[p(z) - p_0] + \left(\tilde{\beta}^a_{33} - \frac{2s_{12}\tilde{\beta}^a_{11}}{s_{11}+s_{12}} \right)[N^-_{a0} - N^-_a(z)] + \left(\tilde{\beta}^d_{33} - \frac{2s_{12}\tilde{\beta}^d_{11}}{s_{11}+s_{12}} \right)[N^+_{d0} - N^+_d(z)] + \left(\tilde{\gamma}_{3333} - \frac{2s_{12}\tilde{\gamma}_{1133}}{s_{11}+s_{12}} \right)\frac{d^2\varphi}{dz^2}. \right) \quad (17)$$

Note that the contribution of the electron-phonon coupling [first two terms in Eq. (17)] as well as the flexoelectric effect (the last term) in the local surface displacement can be comparable with the first terms originating from the chemical expansion. Moreover, using the order of magnitude estimate of $\gamma \sim 1 \times 10^{-10}$ C/m, the flexoelectric contribution to the PFM signal is about 12 pm/V.

Using the decoupling approximation in the 1D Poisson equation,

$$\varepsilon_0\varepsilon_{33}\frac{d^2\varphi(\mathbf{r})}{dz^2} = -q(p - p_0 + n_{C0} - n_C + N_{a0}^- - N_a^- + N_d^+ - N_{d0}^+),$$

i.e., neglecting here the flexoelectric term $\gamma_{ij33}d^2u_{ij}/dz^2$, and regarding that $(-p_0 + n_{C0} + N_{a0}^- - N_{d0}^+) = 0$ due to the electroneutrality in the bulk MIEC, Eq. (17) can be simplified as

$$u_3(z=0) \approx -\int_0^h dz\{\lambda(\tilde{\Xi}^C,\tilde{\gamma})[n_C(z) - n_{C0}] + \lambda(\tilde{\Xi}^V,-\tilde{\gamma})[p(z) - p_0] + \mu(\tilde{\beta}^a,\tilde{\gamma})[N_a^-(z) - N_{a0}^-] + \mu(\tilde{\beta}^d,-\tilde{\gamma})[N_d^+(z) - N_{d0}^+]\}. \quad (18)$$

It is seen from Eq. (18) that the MIEC surface displacement is proportional *to the total charge of each species*. Thus only the injected charges control the displacement. Note that the relation between the total charge and electrostatic potential on the semiconductor surface is well established.[74]

In Eq. (18) we introduced the designations for the flexo-electrochemical coupling constants as

$$\lambda(\tilde{\Xi},\tilde{\gamma}) = \tilde{\Xi}_{33} - \frac{2s_{12}\tilde{\Xi}_{11}}{s_{11}+s_{12}} + \left(\tilde{\gamma}_{3333} - \frac{2s_{12}\tilde{\gamma}_{1122}}{s_{11}+s_{12}}\right)\frac{q}{\varepsilon_0\varepsilon_{33}}, \quad (19)$$

$$\mu(\tilde{\beta},\tilde{\gamma}) = -\tilde{\beta}_{33} + \frac{2s_{12}\tilde{\beta}_{11}}{s_{11}+s_{12}} + \left(\tilde{\gamma}_{3333} - \frac{2s_{12}\tilde{\gamma}_{1122}}{s_{11}+s_{12}}\right)\frac{q}{\varepsilon_0\varepsilon_{33}}, \quad (20)$$

where the first terms originate from the deformation potential or Vegard tensors, while the last ones originate from the flexoelectric coupling.

The flexoelectric effect contribution to the coupling constants λ and μ from Eqs. (19) and (20) is estimated in Table I. It is seen from the Table I that the flexoelectric contribution ranges from 0.1 to 10 eV for crystalline dielectrics, which is comparable to or much higher than the chemical expansion and deformation potential contributions, which are ~0.5−5 eV for ionics. For incipient ($SrTiO_3$) and normal [$Pb(Zr,Ti)O_3$ and $BaTiO_3$] ferroelectrics the flexoelectric effect contribution is much higher than the other ones.

For numerical estimations, we consider the situation when the MIEC film with *mobile acceptors* and *holes* is at thermodynamic equilibrium (i.e., all currents are absent). The analytical solution for acceptor and hole redistribution in a thick MIEC film and its surface displacement are derived in the Appendix assuming that the film thickness $h \gg R_S$, where the screening radius $R_S = \sqrt{\varepsilon_{33}\,\varepsilon_0 k_B T/2p_0q^2}$.

Substitution of the total charge of each species in Eq. (18) in the limit $h \gg R_S$ gives the estimations for the MIEC surface displacement. Note that for the ionically blocking planar top and substrate electrodes the identity $\int_0^h dz[N_a^-(z,t) - N_{a0}^-] = 0$ is valid,[77–79,93] since the total amount of ionized acceptors is conserved. Thus only the electron subsystem contributes to the surface displacement (18) for the ion-blocking electrodes as

$$u_3(V_0) \approx \lambda(\tilde{\Xi}^V,-\tilde{\gamma})\sqrt{\frac{2\varepsilon_{33}\varepsilon_0 k_B T}{q^2}N_{a0}^-}\left[1-\exp\left(-\frac{qV_0}{2k_BT}\right)\right], \quad h \gg R_S, \quad (21a)$$

$$u_3(V_0) \approx \lambda(\tilde{\Xi}^V,-\tilde{\gamma})\sqrt{\frac{\varepsilon_{33}\varepsilon_0 k_B T}{2q^2}N_{a0}^-}\frac{qV_0}{k_BT}, \quad h \gg R_S, \quad |qV_0| \ll k_BT. \quad (21b)$$

It follows from Eq. (21b) that in the linear approximation the electronic surface displacement is proportional to the applied voltage V_0, the stoichiometric acceptor concentration N_{a0}^-, the tensorial deformation potential $\tilde{\Xi}_{ij}^V$, and the flexoelectric effect $\tilde{\gamma}_{iijj}$ via the coupling constant $\lambda(\tilde{\Xi}^V,\tilde{\gamma})$.

Correspondingly, even though the strain contribution can be neglected when considering the chemical potentials and carrier distribution for a film with ion-blocking interfaces, we could not neglect the deformation potential and flexoelectric effect influence on the elastic subsystem, since it is the only source of strain in the case. Measurements of the MIEC surface displacement placed between thin ionically blocking planar electrodes can be performed by an interferometer.

For ionically conducting electrode(s) substitution of the total charge of each species in Eq. (18) yields the mixed ionic-electronic strain-voltage response as

$$u_3(V_0) \approx -\left\{\lambda\left(\tilde{\Xi}^V,-\tilde{\gamma}\right)\sqrt{\frac{2\varepsilon_{33}\varepsilon_0 k_B T}{q^2}N_{a0}^-}\left[\exp\left(-\frac{qV_0}{2k_BT}\right)-1\right] + \mu(\tilde{\beta}^a,\tilde{\gamma})\sqrt{\frac{2\varepsilon_{33}\varepsilon_0 k_B T}{q^2}N_{a0}^-}\left[\exp\left(\frac{qV_0}{2k_BT}\right)-1\right]\right\}. \quad (22)$$

TABLE I. Flexoelectric effect contribution to the coupling constants λ and μ.

Material	Flexoelectric tensor γ (nC/m)	ε (at 300 K)	Flexoelectric coupling constant (eV) $\left(\gamma_{33} - \frac{2s_{12}\gamma_{12}}{s_{11}+s_{12}}\right)\frac{q}{\varepsilon_0\varepsilon_{33}}$	Flexoelectric coupling constant (m^3) $\left(\tilde{\gamma}_{33} - \frac{2s_{12}\tilde{\gamma}_{12}}{s_{11}+s_{12}}\right)\frac{q}{\varepsilon_0\varepsilon_{33}}$	Reference
Crystalline dielectrics, elastomers	~0.01−0.1	~ 10	~0.1−1	~(0.1−1) × 10^{-30}	91
Single-crystal $SrTiO_3$	$\gamma_{3333} = -9$, $\gamma_{1122} = 4$, $\gamma_{1212} = 3$	300	−2	-1.7×10^{-30}	54
Ceramic PZT-5H	$\gamma_{1122} = 500$	2200	~30	~5×10^{-29}	51
Ceramic $BaTiO_3$	$\gamma_{1122} = 10^4$ (with domain walls)	2000	~500	~10^{-27}	52
Single-crystal $BaTiO_3$	$\gamma_{3333} = -0.37$ *ab initio* at 0 K	200	~0.5	~10^{-29}	92

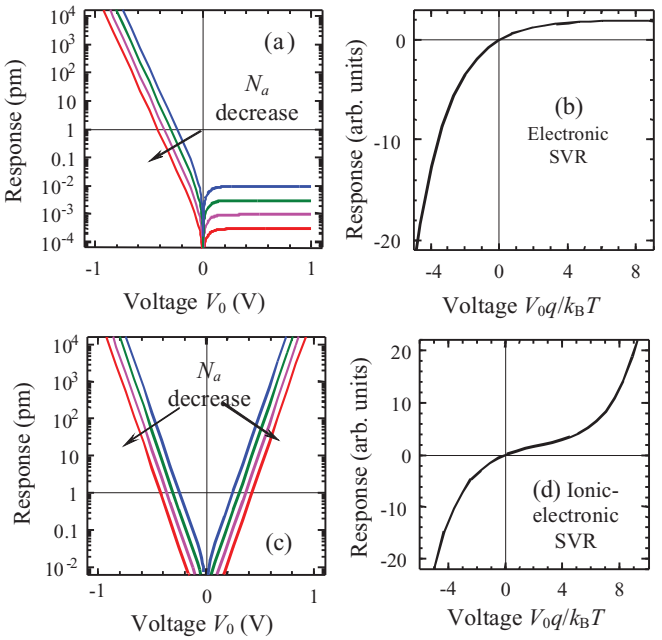

FIG. 2. (Color online) (a),(b) Electronic strain-voltage response (SVR) (absolute value) $u_3(V_0)$ of the MIEC film placed between ionically blocking electrodes. (c),(d) Mixed ionic-electronic strain-voltage response $u_3(V_0)$ of the MIEC film placed between ionically blocking top electrode and ionically conducting bottom electrode calculated for different values of mobile acceptor concentration $N_{a0}^- = 10^{23}$, 10^{24}, 10^{25}, 10^{26} m^{-3} (arrow near the curves), room temperature $T = 300$ K, coupling constants $\lambda(\tilde{\Xi}^V, -\tilde{\gamma}) = 10^{-31}$ m^3 and $\mu(\tilde{\beta}^a, \tilde{\gamma}) = 10^{-30}$ m^3, and MIEC film thickness $h = 100R_S$. (b),(d) are in dimensionless units.

Equation (22) is derived for thick films, $h \gg R_S$. It is seen from Eq. (22) that in the linear approximation the mixed ionic-electronic surface displacement is proportional to the applied voltage V_0, acceptor stoichiometry concentration N_{a0}^-, deformation tensor $\tilde{\Xi}_{ii}^V$, Vegard expansion tensor $\tilde{\beta}_{ii}^a$, and flexoelectric coefficients $\tilde{\gamma}_{iijj}$ via the coupling constants $\lambda(\tilde{\Xi}^V, -\tilde{\gamma})$ and $\mu(\tilde{\beta}^a, \tilde{\gamma})$.

Note that a realistic ESM tip is nano- or submicrosized. Therefore the possibility of the ion motion in the lateral direction rather leads to the condition of an ion-conducting tip electrode than ion blocking.

The electronic strain-voltage response $u_3(V_0)$ of the MIEC film placed between ionically blocking electrodes as calculated from Eq. (21) is shown in Figs. 2(a) and 2(b). The electronic strain-voltage response demonstrates strong asymmetry ("diode-type rectification") with the change of electric voltage polarity: for positive $V_0 > 0$ strong saturation occurs at very small response values, while for negative $V_0 < 0$ the response rapidly increases linearly and reaches noticeable values $u_3(V_0)$ ~1–10 nm at $V_0 \sim 1$ V. Probably nonlinear behavior should be reached for negative voltages in practice since the hole statistics eventually becomes degenerate in the case of strong depletion/accumulation of carriers near the MIEC surface; but the effect of carrier degeneracy is beyond the approximation (21). The origin of the strong voltage asymmetry, shown in Figs. 2(a) and 2(b) is the conservation of the full amount of mobile ionized acceptors, which are negatively charged.

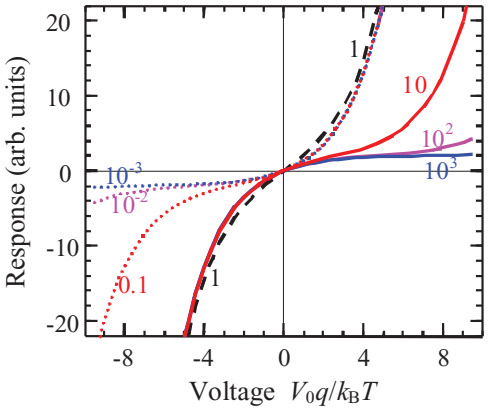

FIG. 3. (Color online) The crossover from the dominantly ionic to electronic strain-voltage response: $|\lambda(\tilde{\Xi}^V, -\tilde{\gamma})/\mu(\tilde{\beta}^a, \tilde{\gamma})| = 0.001, 0.01, 0.1, 1, 10, 100, 1000$ (figures near the curves) Acceptor concentration $N_{a0}^- = 10^{24}$ m^{-3}; other parameters are the same as in Fig. 2.

At negative applied voltage both external negative charges $(-Q_e)$ accommodated at the SPM tip and negatively charged acceptors $(-Q_a)$ accommodate positively charged holes, whose total charge is $Q_p \sim Q_e + Q_a$. At positive applied voltage external positive charges $(+Q_e)$ accommodated at the SPM tip attract the mobile acceptors and repulse the holes, whose total charge in this case is $Q_p \sim Q_a - Q_e$. For the ion-blocking electrodes, the strain response is proportional to the total charge of holes Q_p in accordance with Eq. (21). Thus the oversimplified speculations explain that the response asymmetry for the considered case of the MIEC film with mobile acceptors and holes is at thermodynamic equilibrium. The response's absolute value $u_3(V_0)$ decreases as the ion concentration decreases [follow the arrow direction for the typical values of mobile acceptor concentration $N_{a0}^- = 10^{23}-10^{26}$ m^{-3} in Figs. 2(a) and 2(b)].

The mixed ionic-electronic strain-voltage response $u_3(V_0)$ of the MIEC film placed between telectrodes, one or both of which is ionically conducting, was calculated from Eq. (22) and is shown in Figs. 2(c) and 2(d). In logarithmic voltage scale the asymmetry appearing with the change of electric voltage polarity is rather weak [see Fig. 2(c)]. However, it becomes obvious on the linear scale even for medium applied voltages $0.5 \leqslant |qV_0/k_BT| \leqslant 5$ [see Fig. 2(d)]. The asymmetry effect in Figs. 2(c) and 2(d) originates from the fact that we put $\lambda(\tilde{\Xi}^V, -\tilde{\gamma}) = 0.1\mu(\tilde{\beta}^a, \tilde{\gamma})$ in our calculations, since the typical electronic contribution $\tilde{\Xi}_{ii}^V \sim 10^{-31}$ m^3 is an order of magnitude smaller than the ionic, $\tilde{\beta}_{ii}^a \sim 10^{-30}$ m^3. For the case $\lambda(\tilde{\Xi}^V, -\tilde{\gamma}) = \mu(\tilde{\beta}^a, \tilde{\gamma})$ the asymmetry is absent, as follows from Eq. (22).

The voltage behavior (symmetry or weak asymmetry) of the curves for ionic exchange with ambient follows from the fact that the problem is actually identical to that of the charge accumulation at the interface of an intrinsic semiconductor.[74]

In dimensionless units the strain-voltage response depends on one parameter $qV_0/(k_BT)$, as anticipated from the diode theory for the case $h \gg R_S$ [see Figs. 2(b) and 2(d)].

The crossover from the dominantly ionic ($|\lambda(\tilde{\Xi}^V, -\tilde{\gamma})| \ll |\mu(\tilde{\beta}^a, \tilde{\gamma})|$) to electronic ($|\lambda(\tilde{\Xi}^V, -\tilde{\gamma})| \gg |\mu(\tilde{\beta}^a, \tilde{\gamma})|$) strain-voltage response is shown in Fig. 3. In the case

$|\lambda(\tilde{\Xi}^V, -\tilde{\gamma})| = |\mu(\tilde{\beta}^a, \tilde{\gamma})|$ the strain-voltage curve is symmetric.

V. SUMMARY

We derive the generalized form of the bias-strain-concentration equation describing the linear relation between the concentration of diffusing species and flexoelectric and electronic effects in mixed ionic-electronic conductors. The estimates of the electronic and ionic contributions to the strain-voltage response of the mixed ionic-electronic conductors show that they are of the same order, and hence one cannot neglect the electronic contribution into the surface displacement of the sample with ion-blocking interfaces (injection from the tip). To the best of our knowledge the contribution of the electron-phonon and flexoelectric coupling to the local surface displacement of the mixed ionic-electronic has not been previously discussed. The evolved approach can be extended to treat electrochemically induced mechanical phenomena in solid-state ionics aiming toward analytical theory and phase-field modeling of mixed ionic-electronic conductors.

ACKNOWLEDGMENTS

The authors are grateful to V. Kharton (U. Aveiro) for useful discussions and valuable advice. A.N.M. is very thankful to the referee for important improvements in the paper and calculation details. The research of A.N.M., E.A.E., and L.Q.C. was sponsored in part by the Ukraine State Agency on Science, Innovation and Informatization (Grant No. UU30/004) and the National Science Foundation (Grants No. DMR-0908718 and No. DMR-0820404). This research was supported in part (S.V.K.) by the Materials Science and Engineering Division, Office of Basic Energy Sciences, U.S. DOE. A.K.T. acknowledges the Swiss National Science Foundation for financial support.

APPENDIX: EQUILIBRIUM DISTRIBUTION OF THE POTENTIAL AND SPACE CHARGE IN A SEMI-INFINITE MIEC (DECOUPLING APPROXIMATION)

The equilibrium state corresponds to the absence of ionic (acceptor, donor) and electronic (hole) currents. In the linear drift-diffusion model the acceptor J_a and hole J_p currents have the forms

$$\begin{cases} J_a = -\left(D_a \frac{d}{dz} N_a^- - \eta_a N_a^- \frac{d}{dz}\phi\right) = 0, \\ J_p = -\left(D_p \frac{d}{dz} p + \eta_p p \frac{d}{dz}\phi\right) = 0. \end{cases} \tag{A1}$$

Hereafter we consider that the diffusion coefficients $D_{a,p}$ and mobilities $\eta_{a,p}$ obey the Nerst-Einstein relation $\eta_d/D_d = \eta_n/D_n = q/(k_B T)$, where $k_B = 1.3807 \times 10^{-23}$ J/k, and T is the absolute temperature.

The solution of Eqs. (A1) is

$$N_a^-(z) = N_0 \exp\left(\frac{q\varphi(z)}{k_B T}\right), \tag{A2a}$$

$$p(z) = p_0 \exp\left(-\frac{q\varphi(z)}{k_B T}\right) \tag{A2b}$$

Note, that solutions (A2) coincide with Eqs. (6b) and (8b) as anticipated. Using the decoupling approximation (i.e., neglecting here the term $\gamma_{ij33} d^2 u_{ij}/dz^2$), the boundary problem for electrostatic potential distribution has the following form:

$$\begin{cases} \frac{d^2\phi(z)}{dz^2} = -\frac{q}{\varepsilon_0 \varepsilon}\left[p_0 \exp\left(-\frac{q\phi(z)}{k_B T}\right) - N_0 \exp\left(\frac{q\phi(z)}{k_B T}\right)\right], \\ \phi(0) \approx V_0, \quad \phi(h \to \infty) = 0, \quad E_z = -\frac{d\phi}{dz}\big|_{h\to\infty} = 0. \end{cases} \tag{A3}$$

Rigorously speaking, the approximate equality $\varphi(0) \approx V_0$ in the second line of Eq. (A3) is correct only for *a purely Ohmic tip-electrode–surface contact* for holes (electrons) and in thermodynamic equilibrium, when the gradient of the electrochemical potential level $-\zeta_p \approx e\varphi(z) + k_B T \ln(p(z)/p_0)$ is zero ($\partial\zeta_p/\partial z = 0$) and the potential ζ_p is equal to the Fermi level at the interface [see, e.g., Eqs. (7) and (8) in Ref. 93. In accordance with Refs. 93 and 73, the purely Ohmic contact conditions "correspond to either metal electrodes with adjacent δ-doped semiconductor interfacial layers or heavily doped semiconductor electrodes with a band gap similar to that of the transport layer." When the contact is not Ohmic the "acting" potential difference $\varphi(0)$ is not equal to the applied potential V_0, but to the difference in the electrochemical potentials of the holes divided by their charge q, $\phi(0) = [\xi_p^{\text{tip}} - \xi_p^{\text{MIEC}}(0)]/q$, and the difference $[\xi_p^{\text{tip}} - \xi_p^{\text{MIEC}}(0)]/q$ should be calculated self-consistently from the applied voltage. However the derivation that follows is valid after the ansatz $V_0 \to V_0 + V_b$.

The condition of the potential and electric field vanishing at infinity leads to the local space charge vanishing which is valid under the condition $N_0 = p_0$. Then Eq. (A3) acquires the form

$$\frac{d^2\varphi(z)}{dz^2} = \frac{2qp_0}{\varepsilon_0 \varepsilon} \sinh\left(\frac{q\varphi(z)}{k_B T}\right) \tag{A4}$$

and can be integrated in a straightforward way. Multiplying both sides of the equation by the potential gradient we calculated the first integral as

$$\left(\frac{d\phi(z)}{dz}\right)^2 = \frac{4p_0 k_B T}{\varepsilon_0 \varepsilon}\left[\cosh\left(\frac{q\phi(z)}{k_B T}\right) - a\right],$$

where the constant $a = 1$ from the boundary conditions of the electric field vanishing at the infinity. Using the new variable $u = \cosh[q\phi/(k_B T)]$ one could rewrite (A4) as

$$\phi(z) = \frac{4k_B T}{q} \operatorname{arctanh}\left[\tanh\left(\frac{qV_0}{4k_B T}\right)\exp\left(-\frac{z}{R_S}\right)\right], \tag{A5a}$$

$$N_a^-(z) = p_0 \exp\left(\frac{q\varphi(z)}{k_B T}\right), \quad p(z) = p_0 \exp\left(-\frac{q\varphi(z)}{k_B T}\right). \tag{A5b}$$

Here we introduced the screening radius $R_S = \sqrt{\varepsilon\varepsilon_0 k_B T/(2p_0 q^2)}$.

Substitution of Eqs. (A5b) in Eq. (18) in the limit $h \gg R_S$ gives the estimations for the MIEC surface displacement. Note that for the ionically blocking planar top and substrate electrodes the identity $\int_0^h dz[N_a^-(z,t) - N_{a0}^-] = 0$ is valid,[77–93] since the total amount of ionized acceptors is conserved. The conditions $\int_0^h dz[N_a^-(z,t) - N_{a0}^-] = 0$ and $N_0 = p_0$ lead to the

expression for

$$p_0 = N_0 = N_{a0}^{-}\left[\frac{1}{h}\int_0^h dz\,\exp\left(\frac{q\varphi(z)}{k_BT}\right)\right]^{-1},$$

and thus for the ion-blocking planar electrodes only the electron subsystem contributes to the surface displacement (18) as

$$u_3(z=0) = \lambda(\tilde{\Xi}^V, -\tilde{\gamma})p_0\int_0^h dz\left[1-\exp\left(-\frac{q\varphi(z)}{k_BT}\right)\right]$$
$$\equiv \lambda(\tilde{\Xi}^V, -\tilde{\gamma})hN_{a0}^{-}\int_0^h dz\left(1-e^{q\varphi(z)/k_BT}\right)$$
$$\times\left[\int_0^h dz e^{q\varphi(z)/k_BT}\right]^{-1}. \quad \text{(A6)}$$

Under the condition of high film thickness, $h \gg R_S$, Eq. (A6) reduces to

$$u_3(V_0) \approx \lambda(\tilde{\Xi}^V, -\tilde{\gamma})\sqrt{\frac{2\varepsilon_{33}\varepsilon_0 k_BT}{q^2}N_{a0}^{-}}\left[1-\exp\left(-\frac{qV_0}{2k_BT}\right)\right],$$
$$h \gg R_S, \quad \text{(A7a)}$$

$$u_3(V_0) \approx \lambda(\tilde{\Xi}^V, -\tilde{\gamma})\sqrt{\frac{\varepsilon_{33}\varepsilon_0 k_BT}{2q^2}N_{a0}^{-}}\frac{qV_0}{k_BT}, \quad \text{(A7b)}$$
$$h \gg R_S, \quad |qV_0| \ll k_BT. \quad \text{(A7c)}$$

It follows from Eq. (A7b) that in the linear approximation the electronic surface displacement is proportional to the applied voltage V_0, stoichiometric acceptor concentration N_{a0}^{-}, tensorial deformation potential $\tilde{\Xi}_{ii}^V$ and flexoelectric effect $\tilde{\gamma}_{iijj}$ via the coupling constant $\lambda(\tilde{\Xi}^V, \tilde{\gamma})$.

For ionically conducting electrode(s) substitution of Eqs. (A5) with $p_0 = N_0 = N_{a0}^{-}$ in Eq. (18) yields the mixed ionic-electronic strain-voltage response as

$$u_3(z=0) = -\left\{\lambda(\tilde{\Xi}^V, -\tilde{\gamma})N_{a0}^{-}\int_0^h dz\left[\exp\left(-\frac{q\varphi(z)}{k_BT}\right)-1\right]\right.$$
$$\left.+\lambda(\tilde{\beta}^a, \tilde{\gamma})N_{a0}^{-}\int_0^h dz\left[\exp\left(\frac{q\varphi(z)}{k_BT}\right)-1\right]\right\}. \quad \text{(A8)}$$

Under the condition of thick films, $h \gg R_S$, Eq. (A8) reduces to

$$u_3(V_0)$$
$$\approx -\left\{\lambda(\tilde{\Xi}^V, -\tilde{\gamma})\sqrt{\frac{2\varepsilon_{33}\varepsilon_0 k_BT}{q^2}N_{a0}^{-}}\left[\exp\left(-\frac{qV_0}{2k_BT}\right)-1\right]\right.$$
$$\left.+\lambda(\tilde{\beta}^a, \tilde{\gamma})\sqrt{\frac{2\varepsilon_{33}\varepsilon_0 k_BT}{q^2}N_{a0}^{-}}\left[\exp\left(\frac{qV_0}{2k_BT}\right)-1\right]\right\}. \quad \text{(A9)}$$

*morozo@i.com.ua
†sergei2@ornl.gov

[1] X. Zhang, W. Shyy, and A. M. Sastry, J. Electrochem. Soc. **154**, A910 (2007).
[2] Y. T. Cheng and M. W. Verbrugge, J. Appl. Phys. **104**, 083521 (2008).
[3] V. S. Bagotsky, *Fuel Cells: Problems and Solutions* (Wiley, New York, 2009).
[4] R. O'Hayre, S. W. Cha, W. Colella, and F. B. Prinz, *Fuel Cell Fundamentals* (Wiley, New York, 2009).
[5] A. Magasinski, P. Dixon, B. Hertzberg, A. Kvit, J. Ayala, and G. Yushin, Nat. Mater. **9**, 353 (2010).
[6] C. K. Chan, H. L. Peng, G. Liu, K. McIlwrath, X. F. Zhang, R. A. Huggins, and Y. Cui, Nature Nanotechnol. **3**, 31 (2008).
[7] K. Hirai, T. Ichisubo, T. Uda, A. Miyazaki, S. Yagi, and E. Matsubara, Acta Mater. **56**, 1539 (2008).
[8] T. Mirfakhrai, J. D. W. Madden, and R. H. Baughman, Mater. Today **10**, 30 (2007).
[9] T. E. Chin, U. Rhyner, Y. Koyama, S. R. Hall, and Y. M. Chiang, Electrochem. Solid-State Lett. **9**, A134 (2006).
[10] A. K. Pannikkat and R. Raj, Acta Mater. **47**, 3423 (1999).
[11] A. Morozovska, E. Eliseev, and S. V. Kalinin, Appl. Phys. Lett. **96**, 222906 (2010).
[12] A. Morozovska, E. Eliseev, N. Balke, and S. V. Kalinin, J. Appl. Phys. **108**, 053712 (2010).
[13] N. Balke, S. Jesse, A. N. Morozovska, E. Eliseev, D. W. Chung, Y. Kim, L. Adamczyk, R. E. Garcia, N. Dudney, and S. V. Kalinin, Nature Nanotechnol. **5**, 749 (2010).
[14] N. Balke, S. Jesse, Y. Kim, L. Adamczyk, A. Tselev, I. N. Ivanov, N. J. Dudney, and S. V. Kalinin, Nano Lett. **10**, 3420 (2010).
[15] S. V. Kalinin, B. J. Rodriguez, A. Y. Borisevich, A. P. Baddorf, N. Balke, Hye Jung Chang, Long-Qing Chen, S. Choudhury, S. Jesse, P. Maksymovych, M. P. Nikiforov, and S. J. Pennycook, Adv. Mater. **22**, 314 (2010).
[16] B. J. Rodriguez, S. Choudhury, Y. H. Chu, Abhishek Bhattacharyya, S. Jesse, Katyayani Seal, A. P. Baddorf, R. Ramesh, Long-Qing Chen, and S. V. Kalinin, Adv. Funct. Mater. **19**, 2053 (2009).
[17] S. V. Kalinin, S. Jesse, B. J. Rodriguez, Y. H. Chu, R. Ramesh, E. A. Eliseev, and A. N. Morozovska, Phys. Rev. Lett. **100**, 155703 (2008).
[18] F. C. Larche and J. W. Cahn, Acta Metall. **21**, 1051 (1973).
[19] S. R. Bishop, K. L. Duncan, and E. D. Wachsman, Electrochim. Acta **54**, 1436 (2009).
[20] S. B. Adler, J. Am. Ceram Soc. **84**, 2117 (2001).
[21] A. Y. Zuev, A. I. Vylkov, A. N. Petrov, and D. S. Tsvetkov, Solid State Ion. **179**, 1876 (2008).
[22] H. L. Lein, K. Wiik, and T. Grande, Solid State Ion. **177**, 1795 (2006).
[23] Xiyong Chen, Jinsong Yu, and S. B. Adler, Chem. Mater. **17**, 4537 (2005).
[24] V. V. Kharton, A. V. Kovalevsky, M. Avdeev, E. V. Tsipis, M. V. Patrakeev, A. A. Yaremchenko, E. N. Maumovich, and J. R. Frade, Chem. Mater. **19**, 2027 (2007).
[25] A.Yu. Zuev and D. S. Tsvetkov, Solid State Ion. **181**, 557 (2010).
[26] Y. T. Cheng and M. W. Verbrugge, J. Power Sources **190**, 453 (2009).
[27] X. Zhang, A. M. Sastry, and W. Shyy, J. Electrochem. Soc. **155**, A542 (2008).
[28] F. C. Larche and J. W. Cahn, Acta Metall. **33**, 331 (1985).
[29] F. Yang, Mater. Sci Eng. A **409**, 153 (2005).

[30] A. J. Bard and L. R. Faulkner, *Electrochemical Methods: Fundamentals and Applications* (John Wiley & Sons, New York, 2001).
[31] J. S. Newman, *Electrochemical Systems* (Prentice Hall, Englewood Cliffs, NJ, 1980).
[32] S. W. P. van Sterkenburg, J. Phys. D **25**, 996 (1992).
[33] L. Bjerkan, J. O. Fossum, and K. Fossheim, J. Appl. Phys. **50**, 5307 (1979).
[34] N. F. Foster, J. Appl. Phys. **34**, 990 (1963).
[35] I. Krakovsky, T. Romijin, and A. P. de Boer, J. Appl. Phys. **85**, 628 (1999).
[36] G. Dennler, C. Lungenschmied, N. S. Saricifti, R. Schwodiauer, S. Bauer, and H. Reiss, Appl. Phys. Lett. **87**, 163501 (2005).
[37] C. Herring and E. Vogh, Phys. Rev. **101**, 944 (1956).
[38] J. Liu, D. D. Cannon, K. Wada, Y. Ishikawa, D. T. Danielson, S. Jongthammanurak, J. Michel, and L. C. Kimerling, Phys. Rev. B **70**, 155309 (2004).
[39] J. M. Ziman, *Principles of the Theory of Solids* (Cambridge University Press, Cambridge, 1972), Chap. 6, item 14.
[40] Y. Sun, S. E. Thompson, and T. Nishida, J. Appl. Phys. **101**, 104503 (2007).
[41] J. S. Lim, X. Yang, T. Nishida, and S. E. Thompson, Appl. Phys. Lett. **89**, 073509 (2006).
[42] D. D. Nolte, W. Walukiewicz, and E. E. Haller, Phys. Rev. Lett. **59**, 501 (1987).
[43] R. F. Mamin, I. K. Bdikin, and A. L. Kholkin, Appl. Phys. Lett. **94**, 222901 (2009).
[44] V. S. Mashkevich and K. B. Tolpygo, Zh. Eksp. Teor. Fiz. **31**, 520 (1957) [Sov. Phys. JETP **4**, 455 (1957)].
[45] Sh. M. Kogan, Solid State Phys. **5**, 10, 2829 (1963)
[46] A. K. Tagantsev, Phys. Rev. B **34**, 5883 (1986)
[47] A K. Tagantsev, Phase Transitions **35**, 119 (1991)
[48] A. K. Tagantsev, E. Courtens, and L. Arzel, Phys. Rev. B **64**, 224107 (2001).
[49] W. Ma and L. E. Cross, Appl. Phys. Lett. **79**, 4420 (2001).
[50] W. Ma and L. E. Cross, Appl. Phys. Lett. **81**, 3440 (2002).
[51] W. Ma and L. E. Cross, Appl. Phys. Lett. **82**, 3293 (2003).
[52] W. Ma and L. E. Cross, Appl. Phys. Lett. **88**, 232902 (2006).
[53] W. Ma, Phys. Scr., T **129**, 180 (2007).
[54] P. Zubko, G. Catalan, A. Buckley, P. R. L. Welche, and J. F. Scott, Phys. Rev. Lett. **99**, 167601 (2007).
[55] G. Catalan, L. J. Sinnamon, and J. M. Gregg, J. Phys.: Condens. Matter **16**, 2253 (2004).
[56] G. Catalan, B. Noheda, J. McAneney, L. J. Sinnamon, and J. M. Gregg, Phys. Rev. B **72**, 020102 (2005).
[57] M. S. Majdoub, P. Sharma, and T. Cagin, Phys. Rev. B **77**, 125424 (2008).
[58] S. V. Kalinin, and V. Meunier, Phys. Rev. B **77**, 033403 (2008).
[59] E. A. Eliseev, A. N. Morozovska, M. D. Glinchuk, and R. Blinc, Phys. Rev. B **79**, 165433 (2009).
[60] N. D. Sharma, C. M. Landis, and P. Sharma, J. Appl. Phys. **108**, 024304 (2010).
[61] M. Gharbi, Z. H. Sun, P. Sharma, K. White, and S. El-Borgi, Int. J. Solids Struct. **48**, 249–256 (2011).
[62] J. Y. Li, R. C. Rogan, E. Ustundag, and K. Bhattacharya, Nature Mater. **4**, 776 (2005).
[63] L.Q. Chen, J. Am. Ceram. Soc. **91**, 1835 (2008).
[64] S. Jesse, B. J. Rodriguez, A. P. Baddorf, I. Vrejoiu, D. Hesse, M. Alexe, E. A. Eliseev, A. N. Morozovska, and S. V. Kalinin, Nature Mater. **7**, 209 (2008).
[65] J. L. Ribeiro and L. G. Vieira, Phys. Rev. B **82**, 064410 (2010).
[66] S.Y. Hu and L.Q. Chen, Acta Mater. **52**, 3069 (2004).
[67] B. C. Han, A. Van der Ven, D. Morgan, and G. Ceder, Electrochim. Acta **49**, 4691 (2004).
[68] G. K. Singh, G. Ceder, and M. Z. Bazant, Electrochim. Acta **53**, 7599 (2008).
[69] A. K. Tagantsev, V. Meunier, and P. Sharma, MRS Bull. **34**, 643 (2009).
[70] A. K. Tagantsev, Zh. Eksp. Teor. Fiz. **88**, 2108 (1985) [Sov. Phys. JETP **61**, 1246 (1985)].
[71] W. Ma, Phys. Status Solidi B **247**, 213 (2010).
[72] S. Golmon, K. Maute, S. H. Lee, and M. L. Dunn, Appl. Phys. Lett. **97**, 033111 (2010).
[73] N. W. Ashcroft and N. D. Mermin, *Solid State Physics* (Holt, Rinehart and Winston, New York, 1976).
[74] S. M. Sze, *Physics of Semiconductor Devices*, 2nd ed. (Wiley-Interscience, New York, 1981).
[75] A. I. Anselm, *Introduction to Semiconductor Theory* (Mir, Moscow/Prentice-Hall, Englewood Cliffs, NJ, 1981).
[76] For instance, the well-localized DOS, typical for strongly doped ionic semiconductors, can be modeled as $g_m(x) = (G_m)/(2\Delta_m\Gamma(1+1/k))\exp(-|E_m - x|^k/\Delta_m^k)$ (Γ is the Gamma-function, Δ_m is the half-width, power k>1), while $g_m(x) \sim \sqrt{x}$ corresponds to the Fermi gas.
[77] Y. Gil, O. M. Umurhan, and I. Riess, Solid State Ion. **178**, 1 (2007).
[78] Y. Gil, O. M. Umurhan, and I. Riess, J. Appl. Phys. **104**, 084504 (2008).
[79] Y. Gil, Y. Tsur, O. M. Umurhan, and I. Riess, J. Phys. D **41**, 135106 (2008).
[80] M. M. Rieger, and P. Vogl, Phys. Rev. B **48**, 14276 (1993).
[81] J. F. Nye, *Physical Properties of Crystals: Their Representation by Tensors and Matrices* (Clarendon Press, Oxford, 1985).
[82] J. F. Mitchell, D. N. Argyriou, C. D. Potter, D. G. Hinks, J. D. Jorgensen, and S. D. Bader, Phys. Rev. B **54**, 6172 (1996).
[83] H. F. Tian, J. R. Sun, H. B. Lü, K. J. Jin, H. X. Yang, H. C. Yu, and J. Q. Li, Appl. Phys. Lett. **87**, 164102 (2005).
[84] A. N. Morozovska, E. A. Eliseev, S. L. Bravina, and S. V. Kalinin, e-print arXiv:1008.2389.
[85] S. P. Timoshenko and J. N. Goodier, *Theory of Elasticity* (McGraw-Hill, New York, 1970).
[86] T. Mura, *Micromechanics of Defects in Solids* (Martinus Nijhoff, Boston, 1987).
[87] A. N. Morozovska, S. V. Svechnikov, E. A. Eliseev, and S. V. Kalinin, Phys. Rev. B **76**, 054123 (2007).
[88] A. N. Morozovska, E. A. Eliseev, and S. V. Kalinin, J. Appl. Phys. **102**, 074105 (2007).
[89] F. Felten, G. A. Schneider, J. Muñoz Saldaña, and S. V. Kalinin, J. Appl. Phys. **96**, 563 (2004).
[90] S. V. Kalinin, S. Jesse, B. J. Rodriguez, J. Shin, A. P. Baddorf, H. N. Lee, A. Borisevich, and S. J. Pennycook, Nanotechnology **17**, 3400 (2006).
[91] M. Marvan and A. Havránek, Prog. Colloid Polym. Sci. **78**, 33 (1988).
[92] Jiawang Hong, G. Catalan, J F. Scott, and E. Artacho, J. Phys. Condens. Matter **22** 112201 (2010).
[93] D. B. Strukov, J. L. Borghetti, and R. Stanley Williams, Small **5**, 1058 (2009).